Parasitol Res (2013) 112:3905–3915
DOI 10.1007/s00436-013-3580-3

ORIGINAL PAPER

Morphological and phylogenetic description of a new xenoma-inducing microsporidian, *Microsporidium aurata* nov. sp., parasite of the gilthead seabream *Sparus aurata* from the Red Sea

Kareem Morsy · Abdel Rahman Bashtar · Fathy Abdel-Ghaffar · Saleh Al-Quraishy

Received: 28 July 2013 / Accepted: 12 August 2013 / Published online: 29 August 2013

Abstract A new species of Microsporidia found in the marine teleost *Sparus aurata* collected from Hurghada coasts along the Red Sea, Egypt was described based on light and ultrastructural studies. Twenty three (30.6 %) out of 75 of the examined fish were parasitized with a microsporidian parasite. Numerous macroscopic whitish cysts embedded in the peritoneal cavity were observed to infect many organs of the body including muscles, connective tissues, and the intestinal epithelium. The infection was developed as tumor-like masses of often up to 5 mm in diameter inducing an enormous hypertrophy to the infected organs. Fresh spores appeared mostly ovoid to pyriform in shape reaching a size of 1.7±0.5 (1.5–2.5) μm × 1.3±0.4 (1–2) μm; they possessed a large vacuole at the posterior end. These spores were located within a sporophorous vesicle which was bound by a thick amorphous wall. The ultrastructural features support the placement of the present species within the genus *Microsporidium*. The developmental stages were enclosed within a xenoma structure that was bounded by a double-layered cyst wall. The life cycle of the microsporidian pathogen described herein included four stages: proliferation (merogony), sporogony, sporoblast, spores, and liberation. Mature spores appeared electron dense, uninucleate, and were ellipsoidal in shape. At the anterior end of the spore, the anchoring disk was found in a central position. There was a definite number (5–11) of turns of the polar tube. A 538-bp region of the SSU rDNA gene of the studied species was sequenced (GenBank accession number: KF0220444). Multiple sequence alignment calculated a high degree of similarity (>92 %) with six microsporidian species. The most closely related sequence was provided by the GenBank entry AF151529 for *Microsporidium prosopium* isolated from *Hyperoplus lanceolatus* differing in 67 nucleotide positions in its SSU rDNA with the highest percentage of identity (97.2 %) and the lowest divergence value (0.20). Variations in the morphology of the spores and developmental stages between the two species revealed that the two species are different. The site of infection in the host and description of the onset of parasite development are strong criteria for the placement of the microsporidian parasite of the fish *S. aurata* within the genus *Microsporidium* as a new species, and we propose to name it *Microsporidium aurata* nov. sp.

K. Morsy (✉) · A. R. Bashtar · F. Abdel-Ghaffar
Zoology Department, Faculty of Science, Cairo University, Cairo, Egypt
e-mail: kareemsaid156@yahoo.com

S. Al-Quraishy
Zoology Department, College of Science, King Saud University, Riyadh, Saudi Arabia

Introduction

Microsporidia are common parasites of fish from different geographical areas (Canning and Lom 1986; Lom and Dykova 1992; Sprague et al. 1992; Dykova 1995; Larsson 1999; Shaw and Kent 1999; Lom and Nilsen 2003; Abdel-Ghaffar et al. 2009, 2011). They are eukaryotes with a distinct nucleus and nuclear envelope, but they do not have centrioles or mitochondria and are considered unique among the eukaryotes in that their small subunit ribosomal RNA (SSU-rRNA) genes are smaller than those of typical eukaryotes (Vossbrinck et al. 1993). Cavalier-Smith (1983) included the Microsporidia with other amitochondriate protists, Parabasalia (e.g., *Trichomonas*), Metamonada (e.g., *Giardia*), and Archamoebae (e.g.,

Entamoeba) in the kingdom Archezoa. These protists were presumed to have diverged from other eukaryotes before the acquisition of mitochondria and were suggested as the earliest eukaryotic lineages. Until now, about 90 named species of microsporidia infecting fishes have been established. They were assigned to the genera *Glugea* (Thélohan 1891), *Heterosporis* (Schubert 1969a, b), *Ichthyosporidium* (Caullery and Mesnil 1905), *Loma* (Morrison and Sprague 1981a, b), *Microfilum* (Faye et al. 1991), *Microgemma* (Ralphs and Matthews 1986), *Neonosemoides* (Faye et al. 1996), *Nucleospora* (Hedrick et al. 1991), *Pleistophora* (Gurley 1893), *Spraguea* (Vávrá and Sprague 1976), or *Tetramicra* (Matthews and Matthews 1980). The single record of the genus *Jirovecia* (Weiser 1977) in fish intestine was probably due to a fortuitous ingestion of an infected prey organism. Several species of unclear affinities were included into the collective group *Microsporidium* (Balbiani 1884). Among them, however, only few are xenoma-forming genera of Microsporidia. Little information was available about Microsporidia of genus *Microsporidium* worldwide. Faye (1992) presented sketchy descriptions of 20 unidentified *Microsporidium* spp. from marine fishes collected off the coast of Senegal. In Japan, *Microsporidium* infections in the trunk muscle of farmed yellowtail (Japanese amberjack) *Seriola quinqueradiata* and red seabream *Pagrus major* have caused serious damage to seed production (Egusa 1982; Egusa et al. 1988; Sano et al. 1998). *Microsporidium seriolae* forms elongate whitish nodules in the musculature of yellow- tail, causes liquefaction of muscle fibers resulting in a characteristic concave body surface, and in extreme circumstances, may result in the death of the host fish. Typically, cells containing early stages of parasite development have a simple plasma membrane overlying a region of cytoplasm from which parasites are excluded, within which lies the hypertrophic cell nucleus in the form of a network. Mixed parasitic stages occupy the center of the cell within the nuclear network. The lack of reliable morphological characteristics has made it difficult to identify microsporidia at the species level and to discriminate between related species. Nilsen et al. (1998) showed the genus *Pleistophora* to be polyphyletic, whereas the work of Bell et al. (2001) identified a close relationship between *M. seriolae*, the *Microsporidium* sp. infecting red seabream, and an unidentified *Microsporidium* from Maltese gilthead seabream *Sparus aurata*. Further, Bell et al. (1999) developed a highly sensitive PCR assay for the detection of *M. seriolae*. Recent studies on the phylogeny of the *Microspora* using ribosomal DNA sequence analyses have revealed valuable information about the classification of fish-infecting microsporidians (Nilsen et al. 1998; Lom and Pekkarinen 1999; Bell et al. 2001; Matos et al. 2003). However, the impact of molecular studies has not reduced the importance of classical ultrastructural studies. So, the purpose of the present study was to investigate the accurate position of a new xenoma inducing *Microsporidium* isolated from the gilthead seabream *S. aurata*, a commercially important marine fish of the Red Sea based on morphological and phylogenetic characterization.

Materials and methods

Fish collection and microscopic examination

Samples of 75 individual Gilthead seabream *S. aurata* were collected throughout the whole year of 2012 from the coasts at the Gulf of Suez and Hurghada City of the Red Sea. Fish samples were transported immediately to the Parasitology laboratory at the Zoology Department, Faculty of Science, Cairo University, Egypt using special tanks supplied with aeration and cooling when necessary and were kept alive in a fully prepared aquaria, where they were measured and weighed. Skin surface, fins, and gills were examined by naked eye and with the help of a dissecting microscope for attached parasites, lesions, or external changes. After dissection, microsporidian infection was firstly elucidated by the presence of visible masses embedded in the muscles of the abdominal cavity and along the intestinal wall of the infected fish. These were individually spread on glass microscope slides and pressed under cover slips to the thickness of one cell. Fresh spores were observed under a microscope, and the diameter of the spores was measured as mean ± SD (range) according to the guidelines of Lom and Arthur (1989). Photomicrographs were taken using Zeiss Axiovert 135 microscope equipped by a Canon digital Camera. Prevalence, mean abundance, and morphometric measurements followed the guidelines of Bush et al. (1997). For scanning electron microscopy, specimens of xenoma were fixed in 4 % buffered gluteraldehyde, washed in cacodylate buffer, and dehydrated in ascending alcohol series. After passing through an ascending series of Genosolv-D, they were processed in a critical point drier "Bomer-900" with freon 13 and sputter coated with gold–palladium in a Technics Hummer V and examined with an Etec Autoscan at 20 kV Jeol scanning EM. For TEM, small pieces of the isolated microsporidian cysts were fixed for 48 h in 2.5 % glutaraldehyde in cacodylate buffer at 4 °C for 3 h and then postfixed in 2 % osmium tetroxide in 0.1 M phosphate buffer, pH 7.2 at 4 °C for 2 h. After dehydration in a graded ethanol series, specimens were embedded in Spurr's resin. The semi-thin sections (1 μm thick) were cut on a Leica ultracut (UCT) ultramicrotome and stained with toluidine blue. The ultrathin sections were cut on a Leica UCT ultramicrotome and stained with uranyl acetate and lead citrate. Electron micrographs were made with a Jeol 1220 electron microscope operated at 80 kV.

DNA isolation, PCR, DNA sequencing and phylogenetic analysis

Genomic DNA was extracted from the sporoplasms discharged from spores using the glass bead method described by Undeen and Cockburn (1989). The microsporidians isolated were suspended in an aqueous solution containing 100 mM NaCl, 200 mM sucrose, 10 mM EDTA, and 30 mM Tris–HCl buffer (pH 8.0) to osmotically protect the nuclei from disruption. To this, equal volumes of spore suspension (5×10^{10}) and glass beads (0.425–0.600 μ, 30–40 US Sieve size; Sigma, St. Louis, MO) were added in a 1.5 ml Eppendorf tube. The tubes were vigorously shaken for 1–5 min at a maximum speed on the vortex. When >85 % of the spores had ruptured, as indicated by their dark and empty appearance under a phase contrast microscope, the homogenate was centrifuged at 3,000 r/min for about 2 min and the supernatant solution was transferred to a fresh Eppendorf tube using a Pasteur pipette. Proteinase K (100 μg/ml; Bangalore Genei, Bangalore), one fourth volume of 2.5 % sodium dodecyl sulfate (SDS), 250 mM EDTA, and 500 mM Tris–HCl (pH 9.2) were added, and the mixture was incubated for 1 h at 55 °C to release DNA from the nuclei. The SDS and proteins were precipitated by adding one fifth volume of 1 M potassium acetate, incubated for 1 h at 4 °C, and centrifuged at 5,000 r/min for 20 min. The DNA was precipitated by adding double the volume of cold absolute ethanol. RNA was degraded by digestion with100 μg/ml RNase (Bangalore Genei, Bangalore) for 1 h at 37 °C. DNA concentration and quality was determined both by spectrophotometry at 260 and 280 nm and on 0.8 % agarose gel using a known quantity of λDNA (10 μg/ ml) as a standard before use in subsequent PCRs. A working solution of DNA (10 μg/ml) was prepared in sterile double distilled water.

For PCR amplification, the microsporidian specific primers (Table 1), 18f (5′-CAC CAG GTT GAT TCT GCC-3′) and 1,492r (5′-GGT TAC CTT GTT ACG ACT T-3′) in 20 μl of reaction mixture containing approximately 30 ng template DNA, 0.2 μm of a single primer, 200 μm each dNTP's (Fermentas Life Sciences, Vilnius, Lithuania), and 1 U of Taq DNA polymerase in 1× PCR buffer containing 75 mM Tris–HCl pH 8.8, 20 mM (NH4)2SO4, 0.01 % Tween 20, and 2 mM MgCl2, both provided by the manufacturer of the enzyme (Fermentas Life Sciences, Vilnius, Lithuania). Amplification reactions were carried out for 35 cycles after an initial denaturation for 4 min at 94 °C. Each PCR cycle comprised three steps: denaturation at 94 °C for 50 s, annealing at 56 °C for 50 s, and extension at 72 °C for 80 s with a final extension of 7 min at 72 °C then rested at 4 °C. A negative control without DNA was run in parallel in the same thermocycler. The amplified PCR products were size fractionated by electrophoresis on 1.5 % agarose gel (Gibco-BRL, Grand Island, NY) in 1 Tris–borate–EDTA buffer (89 mM Tris, 89 mM Boric acid, 2 mM EDTA, and pH 8.0), and gels were stained with ethidium bromide (0.5 lg/ml) for 30 min (Sambrook et al. 1989). A standard molecular weight marker (mass ruler DNA ladder, MBI Fermentas) was used in each electrophoretic run and the UV-transilluminated gels were photographed by using Gel Documentation System (Syngene Corporation, Cambridge, UK). The PCR product was then purified on a Qiaquick PCR purification kit (Qiagen Company, CA) and prepared for sequencing. Sequencing was done in ABI 310 automatic DNA sequencer (Applied Biosystems) with the following microsporidian primers: 18f,CACCAGGTTGATTCTGCC;SS350f,CCAAGGA(T/C)GGCAGCAGGCGCGAAA; 350r,TTTCGCGCCTGCTGCC(G/A)TCCTTG;SS530f,GTGCCAGC(C/A)GCCGCGG;SS530r,CCGCGG(T/G)GCTGGCAC;1047r,AACGGCCATGCACCAC;1061f,GGTGGTGCATGCCG and1492r,GGTTACCTTGTTACGACTT. Sequencing templates were prepared using a plasmid preparation kit of Machery-Nagel using the BIO Dye Terminator v 3.1 Ready Sequencing Kit (Applied Biosystems) using universal forward and reverse primers. SSU-rDNA sequences and accession numbers for 16 different microsporidian species were obtained from the NCBI GenBank database and were aligned using the Clustal X program (Thompson et al. 1997) and corrected using the alignment editor BioEdit 4.8.9 (Hall 1999) The resulting sequence fragments were assembled into a single contiguous sequence using the multiple alignment algorithm in Megalign (DNASTAR, Windows version 3.12e). *Antonospora locustae* was included as outgroup. Aligned sequences were analyzed by Maximum Parsimony using PAUP version 3.1b (Swofford 1998). Bootstrap analysis was accomplished using 1,000 neighbor joining replicates.

Results

Light microscopic observations

Twenty three (30.6 %) out of 75 of the gilthead seabream *S. aurata* were parasitized with a microsporidian parasite. Numerous macroscopic whitish cysts embedded in the peritoneal cavity were observed to infect many organs of the body including muscles, connective tissues, and the intestinal epithelium (Figs. 1 and 2). The infection was developed as tumor-like masses often up to 5 mm in diameter inducing an enormous hypertrophy to the infected organs. It was noted that the infection with this parasite is generally increased during winter to 20 % and fall to 10 % in summer. After dissection and rupture of the xenoma, spores were found within the sporophorous vesicle (secondary xenomas) (Figs. 3, 7). Free ellipsoidal spores were identified to belong to the phylum Microsporidia (Figs. 4, 5, 8, 9) reached a size of 1.7±0.5 (1.5–2.5) μm × 1.3±0.4 (1–2) μm. In addition, they possessed

Table 1 Comparison between some previously described species of Microsporidia and *Microsporidium aurata* nov.sp. (present study)

Species	Host	Infection site	Spore			GenBank acc. no.	Divergence	Identity (%)
			Length	Width	Form			
Pleistophora typicalis	*Myoxocephalus scorpious*	Striated muscle	4.4–7.5	2.3–3.0	Microspores uninucleated, macrospores binucleated	AJ252956	7.7	90.0
Pleistophora aegyptiaca	*Saurida tumbil*	Peritoneal cavity	1.7±0.6 (1.5–2.7)	1.5±0.3 (1.2–1.8)	Elongated ,ovoid, or ellipsoidal	JF514548	7.7	90.0
Glugea stephani	*Pleuronectes americanus*	Liver tissue	3.9	1.7	Oblong-ovate, slightly attenuated at the anterior end	AF056015	10.9	90.0
Glugea anomala	*Gasterosteus aculeatus*	Spleen, kidney, peritoneal cavity, subcutaneously	4.9 (4.5–5.5)	2.6 (2.4–2.8)	Elongated, ovoid	AF044391	10.3	90.4
Loma psittaca	*Colomesus psittacus*	Adherent to the intestinal mucosa	4.2±0.4	2.8±0.4	Disporoblastic ovoid spores	FJ 843104	14.6	87.6
Tetramicra brevifilum	*Scophthalmus maximus*	The conjunctiva layers of muscle surface	3.7±0.03	2.7±0.03	Ovoid, wider at the posterior end	AF364303	3.9	95.0
Spraguea lophii	*Lophius piscatorius*	Spinal column close to kidney	–	–	Cylindrical spores are binucleated, whereas oval spores are uninucleated	AF033197	6.9	92.0
Heterosporis anguillarum	*Anguilla japonica*	Skeletal muscle	1.5–2	–	Elongated with a large posterior vacuole filled with dense floccular material	AF387331	9.9	89.7
Microgemma caulleryi	*Hyperoplus lanceolatus*	Liver tissue	2.6 (2.3–2.9)	1.2 (1.1–1.4)	Ovoid and uninucleated	AY033054	5.3	93.7
Microgemma tincae	*Symphodus tinca*	Liver tissue	–	–	Ovocylindrical	AY651319	5.3	93.7
Microsporidium prosopium	*Prosopium williamsoni*	Skeletal musculature	5.6 (5–7)	3.2 (3–4)	Uninucleate, ovoid to pyriform	AF151529	0.2	97.2
Microsporidium seriolae	*Seriola quinqueradiata*	Muscle fibers				AJ295322	1.6	95.0
Kabatana newberryi	*Eucyclogobius newberryi*	Musculature	2.8±0.3	1.9±0.4	Ovoid	EF202572	2.8	93.4
Microsporidium aurata nov.sp.(present study)	*Sparus aurata*	Muscles, connective tissue of ovaries and the intestinal epithelium	1.7±0.5 (1.5–2.5)	1.3±0.4 (1–2)	Ovoid to pyriform	KF0220444	–	–

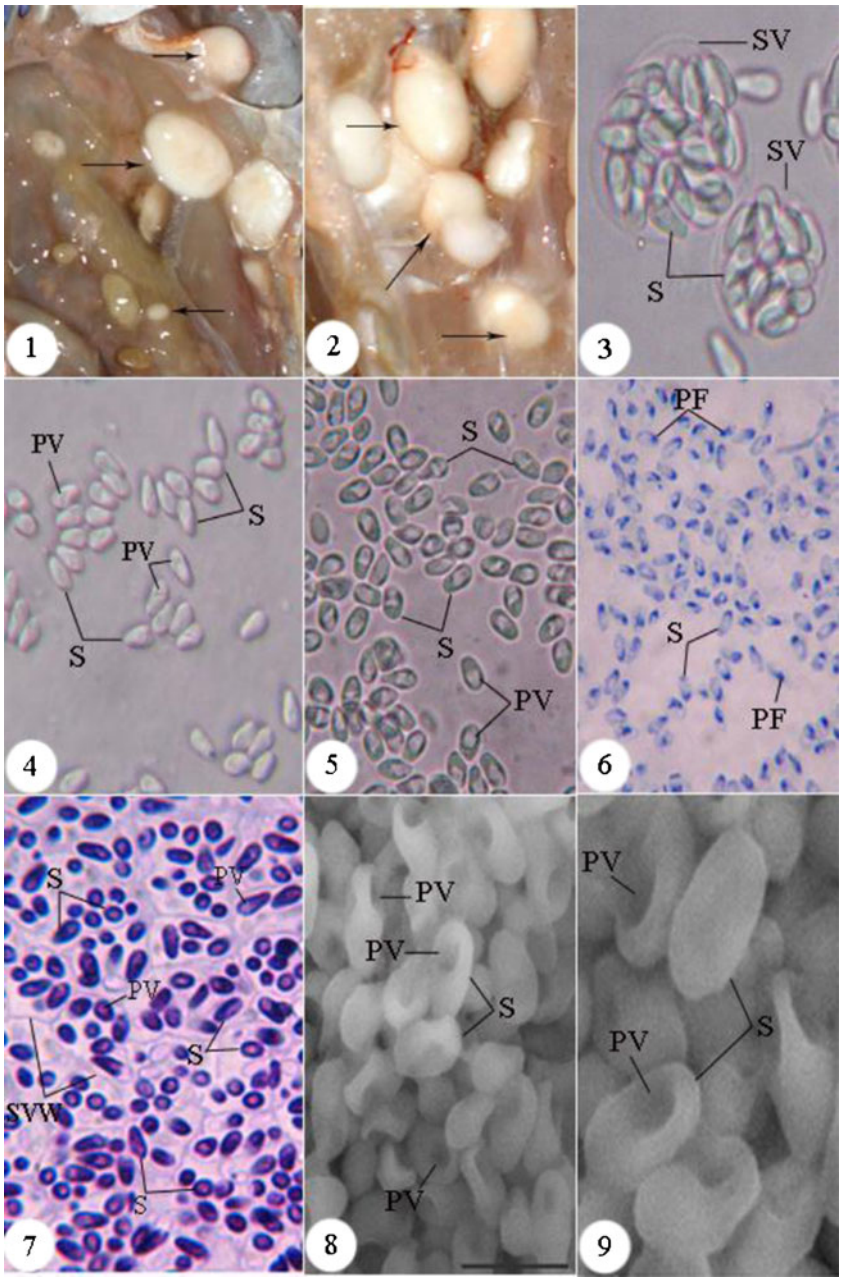

Figs. 1–9 *1*, *2* Photographs of *Sparus aurata* infected with the microsporidian parasite *Microsporidium aurata* n. sp. The infection appeared in the form of whitish cysts (*arrows*) embedded in the viscera of peritoneum. *3–7* Photomicrographs of *3–5* unfixed, fresh spores (*S*) released after rupture of cysts, they are mostly included within special structures known as sporophorous vesicle (*SV*) (Fig. *3* ×2,700). A posterior vacuole (*PV*) is observed situated away from the spore apex (Figs. *4*, *5* ×2,100). (*6*) Giemsa stained smears of spores (*S*) showing the dark staining of polar filaments (*PF*)× 1,500. *7* A semi-thin section through a part of xenoma stained with toluidine blue. Note that each group of spores (*S*) is limited by the walls of sporophorous vesicle (*SVW*) ×2,300. *8*, *9* Scanning electron micrographs of the ellipsoidal spores (*S*) with their posterior vacuoles (*PV*) 8× 5,000 and ×7,500

a large vacuole at the posterior end (Figs. 4, 5). The polar filament may be ejected out of the spore or coiled within it; they were darkly stained with Giemsa (Fig. 6).

Electron microscopic studies

Transmission electron microscopy of the recorded parasite herein revealed that the developmental stages were enclosed within a xenoma structure that was bounded by a double layered cyst wall (Fig. 10). Ultrastructural features support allocation to the genus *Microsporidium* (Ralphs and Matthews 1986). The sporoplasm of generative cells (Fig. 11) developed and formed proliferative cells referred to as meronts which were roundish cells encircled by a typical unit membrane. The uninucleated meronts have a large nuclear region with a single nucleus (Fig. 12) divided to produce binucleated meronts with two spherical nuclei (Fig. 13). Additional multinucleated meronts with six to 12 irregularly shaped nuclei arose by plasmotomy constantly producing new sporonts, the cell that produces the sporoblasts (Figs. 14–16). The next step was the detachment of the plasmalemma of the sporont from the sporophorous vesicle wall (Fig. 17). This space became filled with a fine granular substance containing strands of

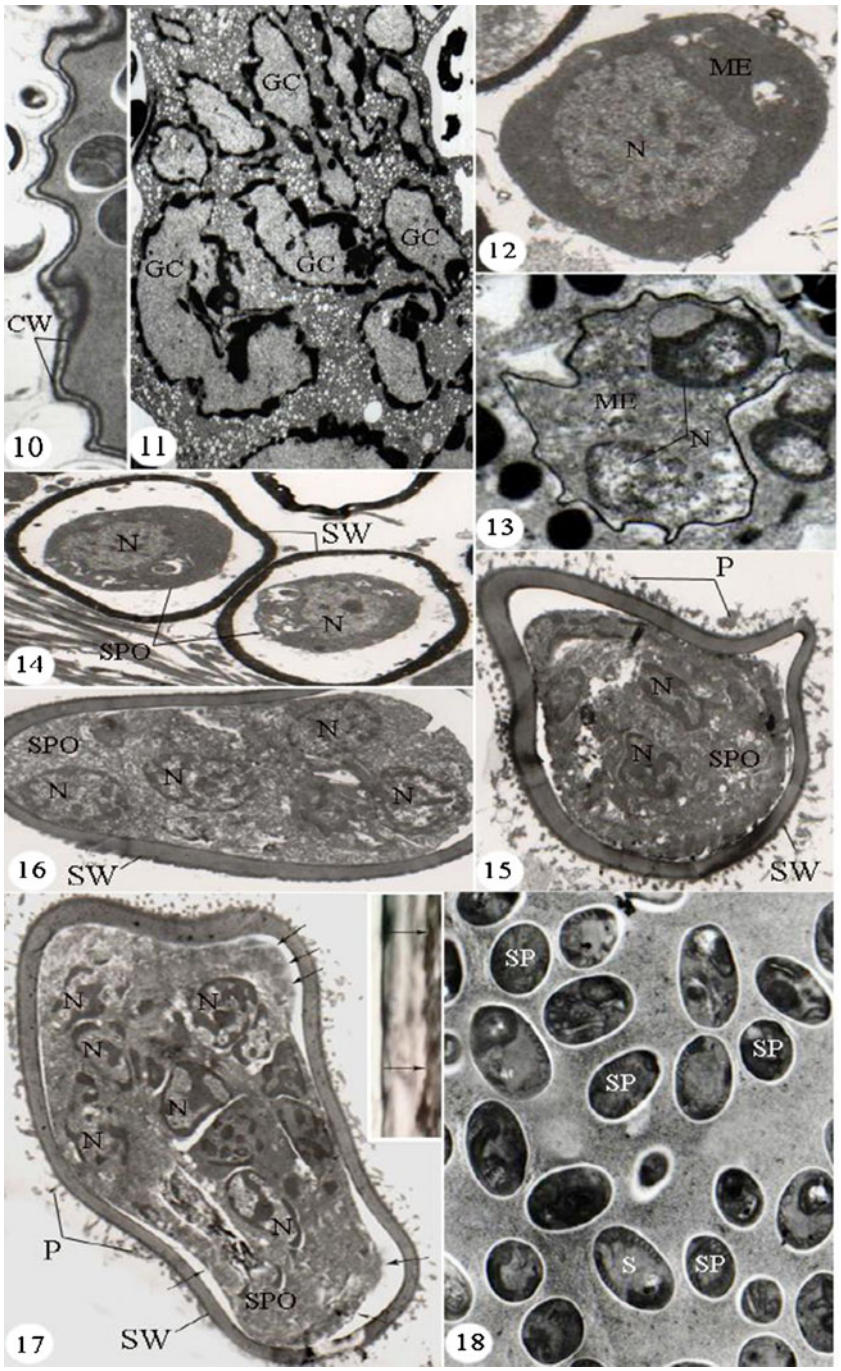

Figs. 10–18 Transmission electron micrographs showing the process of merogony and sporogony. *10* Periphery of a xenoma showing the surrounding double layered cyst wall (*CW*) ×8,000. *11* Generative cells (*GC*) ×3,500. *12* and *13* Meronts (*Me*) with one (uninucleate meront, Fig. *12* ×4,000) or two (binucleate meront, Fig. *13* ×3,400) nuclei (*N*). *14* Uninucleated sporonts (*SPO*) surrounded by sporophorous wall (*SW*) ×6,000. *15* and *16* Multinucleated sporonts (*SPO*) surrounded by the sporophorous wall (*SW*) with many irregular projections (*P*) ×7,000 and ×6,000. *17* A multinucleated sporont (*SPO*) with its plasmalemma (*arrows*) detached from the sporophorous wall (*SW*). Note the temporarily thick irregular projections (*P*) surrounding sporont. ×8,000. *18* A section of xenoma showing sporoblasts (*SP*) and spores (*S*) ×6,800

the endoplasmic reticulum. The sporont segmented into separate sporoblasts (Fig. 18). Sporoblasts are cells that mature and transform into spores without further division but involve a general progressive increase in cytoplasmic density as more ribosomes and endoplasmic reticulum are formed (Figs. 19, 20). Sporogenesis began with the concurrent formation of the exospore and polar filament followed by cell elongation (Figs. 21, 22). The outermost layer, the exospore, is electron dense and has some ridges on its outer surface, while the endospore is much thinner than the exospore (Figs. 22, 23). Mature spores appeared electron dense, uninucleate, and were ellipsoidal in shape (Figs. 23, 24). At the anterior end of the spore, the anchoring disk was found in a central position (Fig. 25). There was a definite number (5–11) of turns of the polar tube (Figs. 26–29). These turns circled around the large future posterior vacuole (Figs. 26, 27). The polaroplast consisted of an anterior region of closely packed membranes and a posterior region comprised a series of loosely packed membranes. All these stages of the parasite are

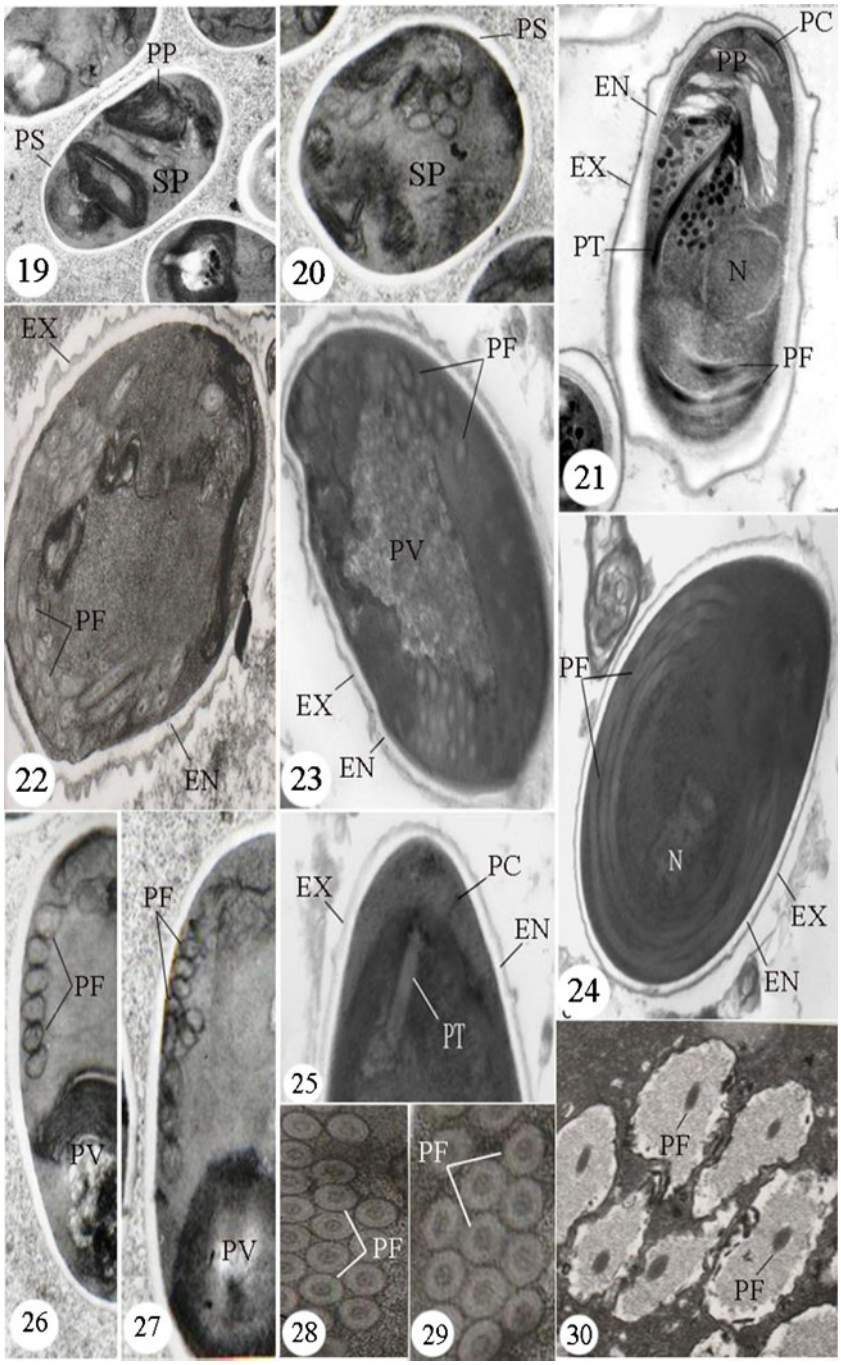

Figs. 19–30 Transmission electron micrographs showing the process of spore maturation. *19* and *20* Sporoblasts (*SP*) within parasitophorous vacuole (*PS*), they are poorly developed and with a lamellar polaroplast (*PP*) and few coils of polar filament (*PF*) ×15,000 and ×20,000. *21* An immature spore surrounded by an outer thick exospore (*EX*) and an inner thin endospore (*EN*). The extrusion apparatus formed of a polar cap (*PC*) covering a polar tube (*PT*) followed by polar filament coils (*PF*) ×20,000. *22–24* Nearly mature spores, they are uninucleated (*N*), the posterior vacuoles are not formed yet but completely formed filament coils are observed ×22,000. *25* Spore apex with the extrusion apparatus composed of the anchoring disk or polar cap (*PC*) which is formed of a cap-like structure that plugged the anterior portion of the spore ×24,000. *26* and *27* High magnifications of mature spores showing the polar filament coils (*PF*) arranged in one row at each side of the posterior vacuole (*PV*) ×20,000 and ×22,000. *28* and *29* High magnifications showing details of the filament coils (*PF*), each coil consists of three layers, an outer, inner dense layers, and a middle lighter one ×30,000 and ×32,000. *30* Transverse sections through polar filaments (*PF*) of mature spores showing the process of autoinfection ×22,000

haplokaryotic and develop in a parasitophorous vacuole bounded by a single membrane in contact with host cell cytoplasm. In cross sections, the polar filament appeared to be divided into three regions (Figs. 28, 29, 30). It has an outer electron dense layer with ridges on its inner surface projecting into an electron transparent layer, with the innermost region of the polar filament filled with an amorphous material of varying electron densities. The possibility of the autoinfection of the same host existed when the polar tube became extruded (Fig. 30).

rDNA sequence comparison

A 538-bp region of the SSU rDNA gene of the studied species was sequenced (GenBank accession number: KF0220444). Multiple sequence alignment calculated the percentages of identities (number of base differences/total number of bases) between the present novel sequence and a range of other microsporidia predominantly from aquatic hosts which demonstrated a high degree of similarity (>92 %) with six microsporidian species (Table 1). These were *Microsporidium prosopium* (97.2 %,

accession no. AF151529), *Microsporidium seriolae* (95.0 %, accession no. AJ295322), *Tetramicra brevifilum* (95.0 %, accession no. AF364303), *Kabatana newberryi* (93.4 %, accession no. EF202572), *Microgemma tincae* (93.7 %, accession no. AY651319), and *Microgemma caulleryi* (93.7 %, accession no. AY033054). The most closely related sequence was provided by the GenBank entry AF151529 for *M. prosopium* isolated from *Hyperoplus lanceolatus* with the highest percentage of identity (97.2 %) and the lowest divergence value (0.20). Phylogenetic analysis of the 16S rDNA sequence (Fig. 31) placed the present microsporidian infecting *S. aurata* within a clade containing one *Kabatana* species (Lom et al. 2001) and two species infecting muscle of yellowtail *Seriola quinqueradiata* and red seabream *Pagrus major* in Japan which were assigned to the collective genus *Microsporidium* (Bell et al. 2001).

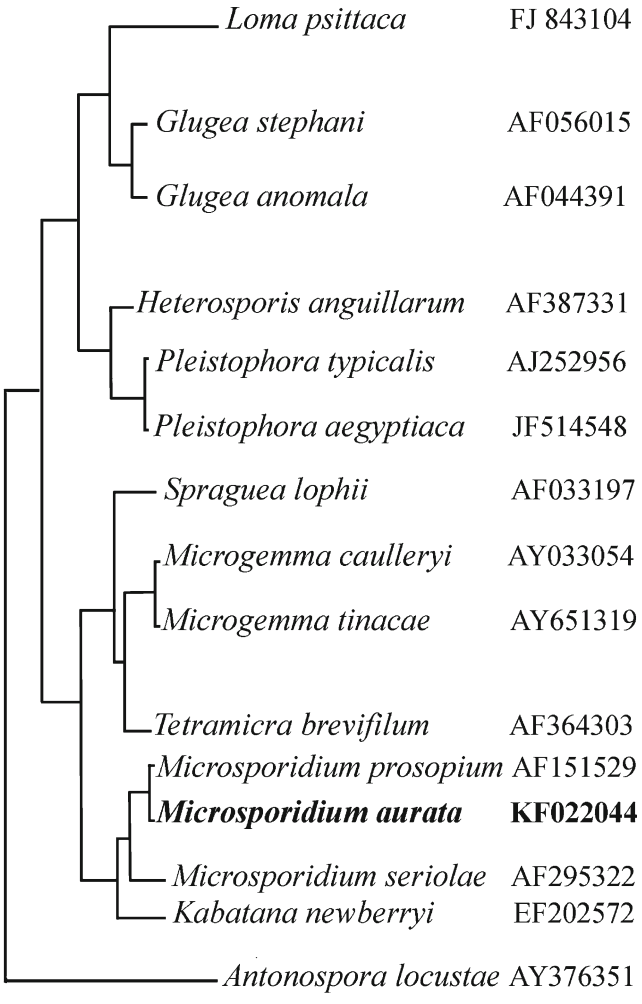

Fig. 31 A phylogenetic tree representing the relationship of *Microsporidium aurata* nov. sp. to other microsporidian species obtained from GenBank

Discussion

In fish, a type of host–parasite relationship involving microsporidia is often characterized by the production of a xenoma (Canning 1976; Weissenberg 1976; Matos et al. 2003; Abdel-Ghaffar et al. 2012; Morsy et al. 2012). This complex structure is defined by the formation of a single hypertrophic host cell in the cytoplasm of which the microsporidian developed and proliferated containing intracellular microsporidian parasites (Weissenberg 1949, 1968, 1976; Canning 1976; Dyková and Lom 1978). The most important characteristics of the spores such as their shape, wall, polaroplast, polar filament, and posterior vacuole are used to distinguish microsporidia from other taxonomic groups (Sprague et al. 1992). The results of the present study demonstrate that the ultrastructure of the spore found in the xenoma of *S. aurata* corresponds to that of the phylum Microsporidia (Vávra and Larsson 1999). One hundred fifty-six microsporidian species were recorded infecting fish that are categorized as 14 genera (Azevedo and Matos 2002; Lom and Nilsen 2003). The followings are those inducing xenomas: *Glugea* (Thélohan 1891), *Ichthyosporidium* (Caullery and Mesnil 1905), *Loma* (Morrison and Sprague 1981a, b), *Microfilum* (Faye et al. 1991), *Microgemma* (Ralphs and Matthews 1986), *Nosemoides* (Vinckier 1975), *Spraguea* (Vávrá and Sprague 1976), and *Tetramicra* (Matthews and Matthews 1980) and *Amazonspora* was added to these (Azevedo and Matos 2003). All of them possess distinctive characteristics which are not recorded in the parasite under study. *Glugea* sp. differs from the present parasite in that its xenoma has an extensive periodic acid-silver methenamine-positive surface coat covering the plasma membrane. The surface of this membrane is amplified by the presence of numerous folds and fine tubular extensions. The plasmalemma gave rise to numerous pinocytotic vesicles which lined the periphery of the xenoma. *Ichthyosporidium* sp. and *Kabatana* sp. differ from current parasite in the arrangement and contents of the developing cells that are in contact with host cells (Lom et al. 2000; Lom 2002) and the absence of xenoma formation in *Kabatana* sp. (Lom et al. 1999, 2000). In *Microgemma* sp. (Ralphs and Matthews 1986) and *Microfilum* sp. (Faye et al. 1991), the life cycles give rise to the formation of xenomas with a microvillous surface which does not occur in the microsporidia described herein. *Amazonspora* possesses a xenoma wall which is composed of up to approximately 22 juxtaposed crossed layers of collagen fibers. *Nosemoides* is characterized by the presence of binucleated spores. The combination of a repent growing habit with a completely entire labellum is the characteristic feature distinguishing the genus *Tetramicra*. In *Spraguea* spp., no sporont stages were observed since the schizontes evolve directly to sporoblastes (Mansour et al. 2012). The microsporidian described above is obviously similar to

Microsporidium arthuri (Lom et al. 1990) recorded from the freshwater fish *Pangasius sutchi*; the spores are identical in shape and only insignificantly different in size and also possess an exospore raised in an irregular mosaic of fields (Lom et al. 1990). Also, it resembled *Microsporidium brevirostris* recorded from *Brachyhypopomus brevirostris* in the development of xenomas which possessed a wall with an irregular surface and is formed of concentric laminated structures spaced by electron lucent layers intermingled with layers of the compressed cell coat (possibly fibroblasts) which forms an electron dense substance and the presence of an isofilar polar filament consisted of a regular coil in a single layer with 9–10 turns surrounding the posterior vacuole. Also, *Microsporidium takedai* (Awakura 1974) recorded from lesions in trunk muscles of cultured salmonids of the genera *Oncorhynchus*, *Salmo*, and *Salvelinus* in Hokkaido, Japan, has spores of shape and size very similar to the present parasite. Other features agree too; however, according to both Awakura (1974) and Miki and Awakura (1977), the species forms cylindrical multinucleate meronts which divide into uninucleate cells. These cells transform directly into sporonts producing sporoblasts by binary fission. Some unique features characterizing the present parasite are the presence of isofilar projections released from the wall of the sporonts, the formation of sporophorous vesicles encircling 10–15 spores, and the process of autoinfection which is marked by the extrusion of polar filament coils agrees with Matos et al. (2003) who suggest that the polar filament of the mature spore pierce through any of the microsporidian life-cycle stages, as well as into the xenoma wall, surrounding in their path the host tissues, as it occurs with other different microsporidian species. This explains the occurrence of all microsporidian life-cycle stages found simultaneously in the same xenoma seems to be the result of autoinfection. PCR-based techniques such as RAPD and SSUrDNA sequence analysis and phylogenetic reconstruction provide DNA markers and sequences, which are found to be more reliable in distinguishing and classifying various organisms (Morrison and Sprague 1981a, b; Kawakami et al. 1992; Vossbrinck et al. 1993; Baker et al. 1994, 1995; Hatakeyama et al. 1997, 2000; Hung et al. 1998; Raynaud et al. 1998; Muller et al. 2000; Tsai et al. 2003; Rao et al. 2004, 2005, 2007; Refardt et al. 2008; Liu et al. 2013). So, analysis of sequence data provided strong genetic evidence that the microsporidium infecting *S. aurata* belonged to the genus *Microsporidium*. Our molecular investigations revealed a close taxonomic relationship between *M. aurata* and *M. prosopium* (97.2 %) differing in 67 nucleotide positions in its SSU rDNA sequence. There are some variations in the morphology of the spores and developmental stages between our novel species and *M. prosopium* as the pattern of sporoblast formation (i.e., detachment of the plasmalemma of the sporont from the sporophorous vesicle wall and filling the space with a fine granular substance containing strands of the endoplasmic reticulum followed by sporoblast formation), the number of polar filament coils (5–11 turns of the polar tube in contrast to 13–16 in *M. prosopium*), and the presence of a double layered cyst wall encircling xenoma. Our results clearly demonstrate the importance of using classical ultrastructural information in combination with molecular data when describing novel parasites (Baker et al. 1995; Weiss 2001). The site of infection in the host and description of the onset of parasite development are strong criteria for the placement the microsporidian parasite of the fish *S. aurata* within the genus *Microsporidium* (Balbiani 1884) as a new species, and we propose to name it *Microsporidium aurata* n. sp. Details of some previous descriptions of the spores of different species are given in Table 1.

Diagnosis of *Microsporidium aurata* nov. sp.

Locality Hurghada coasts, Red Sea (prevalence: 23 (30.6 %) out of 75); host and site of infection: gilthead seabream *S. aurata* (Linnaeus 1758); infecting many organs of the body including muscles, connective tissues, and the intestinal epithelium as macroscopic whitish xenomas up to 5 mm.

Development All developmental stages were uninucleated.

Merogony Multinucleate meronts divide by plasmotomy and enter directly to sporogony.

Sporogony Multinucleate sporonts divide by plasmotomy, producing sporoblasts,

Spores Mature spores appeared electron dense, uninucleated, and ellipsoidal in shape with the anchoring disk was found in an anterior central position. There are 5–11 turns of the polar tube. These turns circled around the large future posterior vacuole.

Remarks The site of infection in the host and description of the onset of parasite development (sporogony) are strong criteria for the placement of the microsporidian infecting *S. aurata* in the genus *Microsporidium*. The contention that this is a new species is supported by the ultrastructural features and rDNA phylogenetic analysis.

Acknowledgments The authors extend their appreciation to the Distinguished Scientist Fellowship Program at King Saud University, Saudi Arabia for funding this work. Also, this work is supported by the Faculty of Science, Cairo University, Egypt.

References

Abdel-Ghaffar F et al (2009) Ultrastructure, development, and host–parasite relationship of a new species of the genus *Pleistophora*—a microsporidian parasite of the marine fish *Epinephelus chlorostigma*. Parasitol Res 106:39–46

Abdel-Ghaffar F, Bashtar AR, Mehlhorn H, Al-Rasheid K, Morsy K (2011) Microsporidian parasites: a danger facing marine fishes of the Red Sea. Parasitol Res 108(1):219–225

Abdel-Ghaffar F, Bashtar AR, Morsy K, Mehlhorn H, Al Quraishy S, Al-Rasheid K, Abdel-Gaber R (2012) Morphological and molecular biological characterization of *Pleistophora aegyptiaca* sp. nov. infecting the Red Sea fish *Saurida tumbil*. Parasitol Res 110(2): 741–752

Awakura T (1974) Studies on the microsporidian infection in salmonid fishes. Sci Rep Hokkaido Fish Hatchery 29:1–93

Azevedo C, Matos E (2002) Fine structure of a new species, *Loma myrophis* (Phylum Microsporidia), parasite of the Amazonian fish *Myrophis platyrhynchus* (Teleostei, Ophichthidae). Europ J Protistol 37:445–452

Azevedo C, Matos E (2003) *Amazonspora hassar* n. gen. and n. sp. (Phylum Microsporidia, fam. Glugeidae), a parasite of the Amazonian teleost *Hassar orestis* (fam. Doradidae). J Parasitol 89:336–341

Baker ND, Vossbrink CR, Maddox JV, Undeen AH (1994) Phylogenetic relationships among *Vairimorpha* and *Nosema* species (Microspora) based on ribosomal RNA sequence data. J Invert Pathol 64:100–106

Baker MD, Vossbrinck CR, Didier ES, Maddox JV, Shadduck JA (1995) Small- subunit ribosomal DNA phylogeny of various microsporidia with emphasis on AIDS-related forms. J Eukaryot Microbiol 42: 564–570

Bell AS, Yokoyama H, Aoki T, Takahashi M, Maruyama K (1999) Single and nested polymerase chain reaction assays for the detection of *Microsporidium seriolae* (Microspora), the causative agent of 'Beko' disease in yellowtail *Seriola quinqueradiata*. Dis Aquat Org 37:127–134

Bell AS, Aoki T, Yokoyama H (2001) Phylogenetic relationships among microsporidia based on rdna sequence data, with particular reference to fish-infecting; *Microsporidium* Balbiani 1884 species. J Eukaryot Microbiol 48(3):258–265

Bush AO, Lafferty KD, Lotz JM, Shostak AW (1997) Parasitology meets ecology on its own terms: Margolis et al. revisited. J Parasitol 83: 575–583

Canning EU (1976) Microsporidia in vertebrates: host-parasite relations at the organismal level. In: Bulla LA, Cheng TC (eds) Comparative pathobiology. Biology of the microsporidia, Plenum, New York 1: 137–202

Canning EU, Lom J (1986) The microsporidia of vertebrates. Academic, New York, p 289

Caullery M, Mesnil F (1905) Sur des haplosporidies parasites de poissons marins. C R Soc Biol 58:640–643

Cavalier-Smith T (1983) In Endocytobiology II: Intracellular Space as Oligogenetic (Schenk, H.E.A. and Schwemmler, W.S., ed.), p. 1027–1034, Walter de Gruyter and Co.

Dykova I (1995) Phylum microspora. In: Woo PTK (ed) Fish diseases and disorders. protozoan and metazoan infections. CAB International, Cambridge 1:149–179

Dyková I, Lom J (1978) Tissue reaction to *Glugea plecoglossi* infection by its natural host, *Plecoglossus altivelis*. Folia Parasitol (Praha) 27: 213–216

Egusa S (1982) A microsporidian species from yellowtail juveniles, *Seriola quinqueradiata*, with "Beko" disease. Fish Pathology 16: 187–192 (In Japanese)

Egusa S, Hatai K, Fujimaki Y (1988) Notes on *Microsporidium* species, the etiological agent of "Beko" disease in red sea bream juveniles, *Pagrus major*. Fish Pathology 23:263–267 (In Japanese)

Faye N (1992) Microsporidies des poisons des cotes senegalaises: faunistique, biologie, ultrastructure. Thesis, Universite Montpellier11, Sciences et Techniques du Languedoc

Faye A, Toguebaye BS, Bouix G (1991) *Microfilum lutjani*n.g. n. sp. (Protozoa Microsporida), a gill parasite of the golden African snapper *Lutjanus fulgens* (Valenciennes, 1830) (Teleostei, Lutjanidae): developmental cycle and ultrastructure. J Protozool 38:30–40

Faye N, Toguebaye BS, Bouix G (1996) Ultrastructure and development of *Neonosemoides tilapiae* (Sakiti and Bouix, 1987) n.g., n. comb. (Protozoa, Microspora) from African cichlid fish. Europ J Protistol 32:320–326

Gurley RR (1893) On the classification of Myxosporidia, a group of protozoan parasites infesting fishes. Bull U S Fish Comm 11:407–420

Hall TA (1999) BioEdit: a user-friendly biological sequence alignment editor and analysis program for Windows 95/98/NT. Nucl Acids Symp Ser 41:95–98

Hatakeyama Y, Kawakami Y, Iwano H, Inoue T, Ishihara R (1997) Analysis and taxonomic inferences of small subunit ribosomal RNA sequence of five microsporidia pathogenic to the silkworm, *Bombyx mori*. J Seric Sci Jpn 66:242–252

Hatakeyama Y, Bansal AK, Iwano H, Kawakami Y, Ishihara R (2000) Characterization of SSU-rRNA sequence of a new microsporidium *Nosema* sp. (Nosematidae: Microsporidia), isolated from *Antheraea mylitta* Drury (Lepidoptera: Saturniidae) in India. J Seric 39:131–134

Hedrick RP, Groff JM, Baxa D (1991) Experimental infections with *Nucleospora salmonis* n. g., n. sp.: an intranuclear microsporidium from Chinook salmon (*Onchorhynchus tschawytscha*). Am Fish Soc News 19: 5

Hung HW, Lo CF, Tseyg CC, Peng SE, Chou CM, Kou GH (1998) The small subunit ribosomal RNA gene sequence of *Pleistophora anguillarum* and the use of PCR primers for diagnostic detection of the parasite. J Euk Microbiol 45(5):556–560

Kawakami Y, Inoue T, Kikuchi M, Takayanagi M, Sunairi M, Ando T, Ishihara R (1992) Primary and secondary structures of 5S ribosomal RNA of *Nosema bombycis* (Nosematidae: Microsporidia). J Seric Sci Jpn 61:321–327

Larsson JIR (1999) Identification of microsporidia. Acta Protozool 38: 161–197

Liu H, Pan G, Dang X, Li T, Zhou Z (2013) Characterization of active ribosomal RNA harboring MITEs insertion in microsporidian *Nosema bombycis* genome. Parasitol Res 112(3):1011–1020

Lom J (2002) A catalogue of described genera and species of microsporidians parasitic in fish. Syst Parasitol 53:81–99

Lom J, Arthur JR (1989) A guideline for the preparation of species descriptions in Myxosporea. J Fish Dis 12:151–156

Lom J, Dykova I (1992) Protozoan parasites of fishes. Elsevier, Amsterdam

Lom J, Nilsen F (2003) Fish Microsporidia: fine structural diversity and phylogeny. Int J Parasitol 33:107–127

Lom J, Pekkarinen M (1999) Ultrastructural observations on *Loma acerinae* (Jírovec, 1930) comb. nov. (Phylum Microsporidia). Acta Protozool 38:61–74

Lom J, Dykova I, Shaharom F (1990) *Microsporidiurn arthuri* n. sp. parasite of *Pangasius sutch*i (Pangasiidae, Siluroidea) in South-East Asia. Dis Aquat Org 8:65–67

Lom J, Dyková I, Tonguthai K (1999) *Kabataia* gen. n., a new genus proposed for *Microsporidium* spp. infecting trunk muscles of fishes. Dis Aquat Org 38:39–46

Lom J, Dyková I, Tonguthai K (2000) *Kabatana* gen. n., new name for the microsporidian genus *Kabataia* Lom, Dykova et Tonguthai, 1999. Folia Parasitol (Praha) 47:78

Lom J, Nilsen F, Dyková I (2001) *Thelohania contejeani* Henneguy, 1892: dimorphic life cycle and taxonomic affinities, as indicated by ultrastructural and molecular study. Parasitol Res 87:860–872

Mansour L, Ben Hassine OK, Vivares CP, Cornillot E (2012) *Spraguea lophii* (Microsporidia) parasite of the teleost fish, *Lophius piscatorius* from Tunisian coasts: evidence for an extensive chromosome length polymorphism. Parasitol Int 62(1):66–74

Matos E, Corral L, Azevedo C (2003) Ultrastructural details of the xenoma of *Loma myrophis* (phylum Microsporidia) and extrusion of the polar tube during autoinfection. Dis Aquat Org 54:203–207

Matthews RA, Matthews BF (1980) Cell and tissue reactions of turbot *Scophthalmus maximus* (L.) to *Tetramicra brevifilum* gen.n., sp.n. (Microspora). J Fish Dis 3:495–515

Miki S, Awakura T (1977) The fine structure of *Glugea takedai* Awakura, 1974 (Microsponda, Nosematidae). Sci Rep Hokkaido Fish Hatchery No 32:1–19

Morrison CM, Sprague V (1981a) Electron microscopical study of a new genus and new species of microsporida in the gills of Atlantic cod *Gadus morhua* L. J Fish Dis 4:15–32

Morrison CM, Sprague V (1981b) Microsporidian parasites in the gills of salmonid fishes. J Fish Dis 4:371–386

Morsy K, Abdel-Ghaffar F, Mehlhorn H, Bashtar AR, Abdel-Gaber R (2012) Ultrastructure and molecular phylogenetics of a new isolate of *Pleistophora pagri* sp. nov. (Microsporidia, Pleistophoridae) from *Pagrus pagrus* in Egypt. Parasitol Res 111(4):1587–1597

Muller A, Trammer T, Chioralia G, Seitz HM, Diehl V, Franzen C (2000) Ribosomal RNA of *Nosema algerae* and phylogenetic relationship to other microsporidia. Parasitol Res 86:18–23

Nilsen F, Endresen C, Hordvik I (1998) Molecular phylogeny of microsporidians with particular reference to muscle infecting species of fishes. J Euk Microbiol 45:535–543

Ralphs JR, Matthews RA (1986) Hepatic microsporidiosis due to *Microgemma hepaticus* n. gen., n. sp. in juvenile grey mullet *Chelon labrosus*. J Fish Dis 9:225–242

Rao SN, Muthulakshmi M, Kanginakudru S, Nagaraju J (2004) Phylogenetic relationships of three new microsporidian isolates from the silkworm, *Bombyx mori*. J Invertbr Pathol 86:87–95

Rao SN, Nath BS, Saratchandra B (2005) Characterization and phylogenetic relationships among microsporidia infecting silkworm, *Bombyx mori*, using inter simple sequence repeat (ISSR) and small subunit rRNA (SSUrRNA) sequence analysis. Genome 48: 355–366

Rao N, Nath BS, Bhuvaneswari G, Raje S (2007) Genetic diversity and phylogenetic relationships among microsporidia infecting the silkworm, *Bombyx mori*, using random amplification of polymorphic DNA: morphological and ultrastructural characterization. J Invert Pathol 96:193–204

Raynaud L, Delbac F, Broussolle V, Rabodonirina M, Girault V, Wallon M, Cozon G, Vivares CP, Peyron F (1998) Identification of *Encephalitozoon intestinalis* in travellers with chronic diarrhea by specific PCR amplification. J Clin Microbiol 36:37–40

Refardt D, Decaestecker E, Johnson PTJ, Vavra J (2008) Morphology, molecular phylogeny and ecology of *Binucleata daphniae* n. g., sp. n. (Fungi: Microsporidia), a parasite of *Daphnia magna* Straus, 1820 (Crustacea: Branchiopoda). J Eukaryot Microbiol 55(5):393–408

Sambrook J, Fritsch EF, Maniatis T (1989) "Chapter 14: in vitro amplification of DNA by the polymerase chain reaction", in molecular 133 cloning: a laboratory manual, 2nd edn. Cold Spring Harbor Laboratory, New York

Sano M, Sato J, Yokoyama H (1998) Occurrence of Beko disease caused by *Microsporidiurn seriolae* (Microspora) in hatchery-reared juvenile yellowtail. Fish Pathology 33:11–16

Schubert G (1969a) Ultracytologische Untersuchungen an der Spore der Mikrosporidienart. Heterosporis finki, gen. n., sp. n. Parasitol Res 32:59–79

Schubert G (1969b) Elektronenmikroskopische Untersuchungen zur Sporonten und Sporenentwicklung der Mikrosporidienart Heterosporis finki. Parasitol Res 32:80–92

Shaw RW, Kent ML (1999) Fish microsporidia. In: Wittner M, Weiss LM (eds) The Microsporidia and microsporidiosis. ASM, Washington, DC, pp 502–516

Sprague V, Becnel JJ, Edwin IH (1992) Taxonomy of phylum Microspora. Crit Rev Microbiol 18:285–395

Swofford DL (1998) PAUP* Phylogenetic analysis using parsimony and other methods. V. 4.0 Beta. Sinauer associates, Sunderland

Thélohan P (1891) Sporozoaires nouveaux, parasites des muscles des poissons. C R Acad Biol 3:27–29

Thompson JD, Gibson TJ, Plewniak F, Jeanmougin F, Higgins DG (1997) The CLUSTAL_X windows interface: flexible strategies for multiple sequence alignment aided by quality analysis tools. Nucleic Acids Res 25:4876–4882

Tsai SJ, Lo CF, Soichi Y, Wang CH (2003) The characterization of microsporidian isolates (Nosematidae: Nosema) from five important lepidopteran pests in Taiwan. J Invertbr Pathol 83:51–59

Undeen AH, Cockburn AF (1989) The extraction of DNA from microsporidian spores. J Invertbr Pathol 54:132–133

Vávrá, J, Sprague V (1976) Biology of the microsporidia. In: Bulla, L. A., Jr. & Cheng, T. C. (ed.), Comparative Pathobiology, Plenum Press, New York 1:1–369

Vinckier D (1975) *Nosemoides* gen. n., *N. vivieri* (Vinckier, Devauchelle and Prensier, 1970) comb. nov (Microsporidie): étude de la differenciation sporoblastique et génèse des differentes structures de la spore. J Protozool 22:170–184

Vossbrinck CR, Baker MD, Didier ES, Debrunner-Vossbrinck BA, Shadduck JA (1993) Ribosomal RNA sequences of *Encephalitozoon hellem* and *Encephalitozoon cuniculi*: species identification and phylogenetic construction. J Euk Microhiol 40:354–362

Weiser J (1977) Contribution to the classification of Microsporidia. Vest CS Spol Zool 41:308–320

Weiss LM (2001) Microsporidia Cincinnati. J Eukaryot Microbiol (Suppl.): 475–495

Weissenberg R (1949) Cell growth and cell transformation by intracellular parasites. Anat Rec 103:517–518

Weissenberg R (1968) Intracellular development of the microsporidian *Glugea anomala* in hypertrophying migratory cells of the fish *Gasterosteus aculeatus*, an example of the formation of the xenoma tumors. J Protozool 15:44–57

Weissenberg R (1976) Microsporidian interactions with host cells. In: Bulla LA, Cheng TC (eds) Comparative pathobiology. Biology of the Microsporidia, Plenum, New York 1: 203–237